

Mechanical Properties of Multiwell Sandstone
at 2405-m Depth

Prepared for
Sandia National Laboratories

by

Wunan Lin
Earth Sciences Department
Lawrence Livermore National Laboratory
University of California
P.O. Box 808
Livermore, California 94550

January 1983

Mechanical Properties of Multiwell Sandstone
at 2405-m Depth

Wunan Lin

Introduction

The Multiwell project is the field testing phase of the DOE Western Gas Sands Stimulation Sub-Program. Two wells, 130 ft apart, have been drilled in Garfield County, Colorado (Sec. 34 T6S R94W) to a depth of about 2545 m. They are referred to as MWX-1 and 2. To predict and understand the geometry, intensity, and extent of fracture in the medium around a well in an in situ fracturing test, we need to know the mechanical (Equation of State) properties of the rock. In this informal report we present the laboratory measured mechanical properties of a sandstone from a depth of 2405 m, in Well MWX-1. The mechanical properties included in this report are tensile strength, compressive strength under triaxial compressive loading, stress-strain relations under triaxial compressive loading, and pressure-volume (P-V) behavior under hydrostatic compression. The mechanical properties of a silstone from the 1994-m depth in MWX-1 were reported in a previous informal report (Lin, Nov. 1982).

Starting Material and Specimen Preparation

The core section that we received was a cylindrical core of 10.16 cm diameter and about 18 cm long. The core was classified by others as a sandstone with a grain size of about 0.1 mm. Bedding planes, indicated by roughly lineated black mineral grains, were almost horizontal (normal to the core axis). The core section was light gray in color and appeared quite homogeneous. No additional study on the mineralogical composition of the core was planned.

Right cylindrical specimens of 1.9 cm in diameter with various lengths were cored from the starting core material. The specimens for the determination of compressive strength and stress-strain relations were about 4.2 cm long; the specimens for the measurements of volumetric strain under hydrostatic compression were 2.54 cm long; and the specimens for Brazilian testing (to determine tensile strength) were about 0.9 cm long. The two ends of the specimens were ground and polished to be parallel to within 0.02 mm. The specimens were then dried in a vacuum oven at about 30°C until their weights remained constant for at least one day.

Dry bulk density of each specimen was calculated from its dry weight and its dimensions. The averaged dry bulk density of the sandstone is 2.484 ± 0.009 gm/cc.

To measure the compressive strength, the specimens were jacketed in tygon tubing of 0.32 cm thick between steel end pieces. For the determination of stress-strain relations at confining pressures greater than 10 MPa and the P-V behavior, the specimens were encapsulated in annealed copper jackets of about 0.12 mm thick. Two pairs of electrical resistance strain gauges were mounted on the jacket near the middle of the specimens for both the stress-strain relation and P-V relation determinations to measure longitudinal and radial strains. For the determinations of stress-strain at 0.1 MPa, the strain gauges were attached directly on the rock surface.

Experimental Techniques

The experimental techniques for these measurements were conventional. Briefly, for the determination of tensile strength using the Brazilian test the disc type specimens (1.9 cm diameter, 0.9 cm long) were loaded diametrically until failure. Total load and diametrical displacement (parallel to loading) were recorded on an X-Y recorder. Tensile strength (σ_t) was calculated from the total load (F) by

$$\sigma_t = \frac{F}{\pi RL}$$

where R and L are radius and length of a specimen respectively.

To determine the compressive strength of a specimen as a function of confining pressure, we axially loaded the tygon jacketed specimen (4.2 cm long) until failure, with the confining pressure kept constant. The differential load (axial load minus confining pressure) and axial displacement were recorded on an x-y recorder. The compressive strength was calculated by dividing the differential load at the peak of a load-displacement curve by the cross sectional area of the specimen. To correct the change of the cross sectional area of a specimen due to the axial compressive loading, we assume that all strains are homogeneous and the volume of the specimen remained constant before failure. Therefore, the change of the cross sectional area was linearly proportional to the axial shortening.

To determine the stress-strain relation under triaxial compressive loading, the specimen was loaded the same way as that used in measuring the compressive strength. In this case, the long specimens (4.2 cm long) with attached strain gages (both with and without copper jacket) were loaded axially when confining pressures were kept constant. Differential stress, confining pressure, longitudinal strain, and radial strain were recorded by a computer during the loading and unloading path. We usually loaded the sample until the volumetric strain began to show a positive increment. The specimens were loaded both normal and parallel to bedding. We measured the stress-strain relation at confining pressures from 0.1 MPa to 75 MPa.

The short strain gauged samples (2.54 cm long) were used in determining the volumetric strain under hydrostatic compression. We measured longitudinal

strain (ϵ_l) and radial strain (ϵ_r) as a function of confining pressure up to 0.8 GPa. The volumetric strain (ϵ_v) was calculated as $\epsilon_v = \epsilon_l + 2 \epsilon_r$. For a transversely isotropic rock, as the MWX-1 sandstone seems to be, the volumetric strain so measured on a specimen cored normal to bedding is close to the real volumetric strain under hydrostatic compression.

Results and Discussion

The tensile strengths (σ_t) of the sandstone measured normal and parallel to bedding are shown in Table 1. The tensile strength measured normal to bedding is slightly smaller than that measured parallel to bedding.

Table 1. Tensile Strength of MWX-1 Sandstone, 2405-m Depth, 0.1 MPa.

Rock	Normal (⊥) or Parallel ()	Number of tests	$\sigma_t \pm 1 \text{ sd}$ (MPa)
Sandstone	⊥	13	15.26 ± 0.84
		11	16.91 ± 0.45

The small values of one standard deviation shown in Table 1 indicate that the sandstone is quite homogeneous in its tensile strength and the Brazilian tests give consistent results.

For the purpose of comparison, the tensile strength of MWX-1 siltstone from a depth of 1994 M, reported previously, is shown in Table 2. We see that the sandstone has a tensile strength about 60% greater than the siltstone.

Table 2. Tensile Strength of MWX-1 Siltstone, 1994-m Depth, 0.1 MPa.

Rock	Normal (\perp) or Parallel (\parallel)	Number of tests	$\sigma_t \pm 1 \text{ sd}$ (MPa)
Siltstone	\perp	13	9.42 ± 0.53
	\parallel	5	9.32 ± 0.47

The compressive strength of the MWX-1 sandstone is shown in Figures 1 and 2, as Mohr Circles and Mohr envelopes (dashed line). Figures 1 and 2 are for the specimens loaded normal and parallel to bedding respectively. The intercept of the Mohr envelopes at 0.1 MPa in these two figures give the inherent shear strength (S_0) of the sandstone when loaded normal and parallel to bedding. These are 36 MPa and 28 MPa respectively.

The stress-strain relations of the MWX-1 sandstone are shown in Figures 3 to 12 in terms of differential stress ($\sigma_1 - \sigma_3$) versus strain (ϵ). In these figures, the longitudinal strain (ϵ_L), radial strain (ϵ_r), and volumetric strain (ϵ_v) are shown. Figures 3 to 7 are for the specimens loaded normal to bedding at confining pressures to 75 MPa. Figures 8 to 12 show the stress-strain relation of a specimen loaded parallel to bedding at confining pressures to 75 MPa. The ϵ_v curves show that the volumetric strain reaches a maximum compression before onset of failure. This is shown by an arrow head in these figures. The differential stress corresponding to the maximum volumetric compression is

defined as the long-term strength of the material. The Young's modulus of the sandstone at 50% compressive strength are calculated by the least squares fit. Table 3 lists the Young's modulus, the ultimate strength (from Figures 1 and 2), and the long-term strength (as percent of the ultimate strength) of the MWX-1 sandstone loaded normal and parallel to bedding. Both ultimate strength and long-term strength of the sandstone increase with increasing confining pressure. Young's modulus, on the other hand, increases slightly with increasing pressure then decreases when pressure reaches 50 MPa when loaded normal to bedding and 75 MPa when loaded parallel to bedding. The deformation mode of the sandstone samples at these pressures were probably in the transition from brittle to ductile.

Table 3. Comparison of strength and deformability results for the 2405-m MWX-1 sandstone, normal and parallel to bedding.

Confining Press. (MPa)	Young's Modulus at 50% Ultimate Strength (GPa)		Long Term Strength as % of Ult. Strength		Ultimate Strength (MPa)	
	⊥	//	⊥	//	⊥	//
0.1	40.3	38.4	79.5	83.3	200	204
10	41.4	39.8	80.5	74.2	272	303
20	44.7	39.8	80.4	72.9	320	343
50	42.5	40.1	81.3	79.8	444	481
75	36.3	38.1	80.7	85.0	522	562

For the purpose of comparison, the results of the previously reported compression tests on the MWX-1 siltstone at 1994-m depth are recalled in Table 4. We see that the MWX-1 sandstone at 2405-m depth is stronger and stiffer than the MWX-1 siltstone at 1994-m depth.

Table 4. Comparison of strength and deformability results for the 1994-m MWX-1 siltstone, normal and parallel to bedding.

Confining Press. (MPa)	Young's Modulus at 50% Ultimate Strength (GPa)		Long Term Strength as % of Ult. Strength		Ultimate Strength (MPa)	
	⊥	//	⊥	//	⊥	//
0.1	28.6	25.0	**	80	98.3	85.0
10	28.2	30.8	87	93	196.0	183.6
20	29.9	33.3	86	88	232.0	214.4
50	30.8	35.1	97	91	315.0	291.4
100	--	36.4	--	86	340.0	448.0

* This specimen was from 1996-m depth.

**No long-term strength was observed.

The volumetric strain of the MWX-1 sandstone under hydrostatic compression is shown in Figure 13. The unloading path stays to the right (larger volumetric strain) of the loading path. This is due to inelastic strain of the rock. The residual volumetric strain is about 1%. In the loading path there is a clear decrease of compressibility at a confining pressure of about 40 MPa. This is due to the closing-up of most of the grain boundary microcracks in the specimen.

Fig. 1. Compressive strength of MWX-1 sandstone, 2405-m depth,
loaded normal to bedding

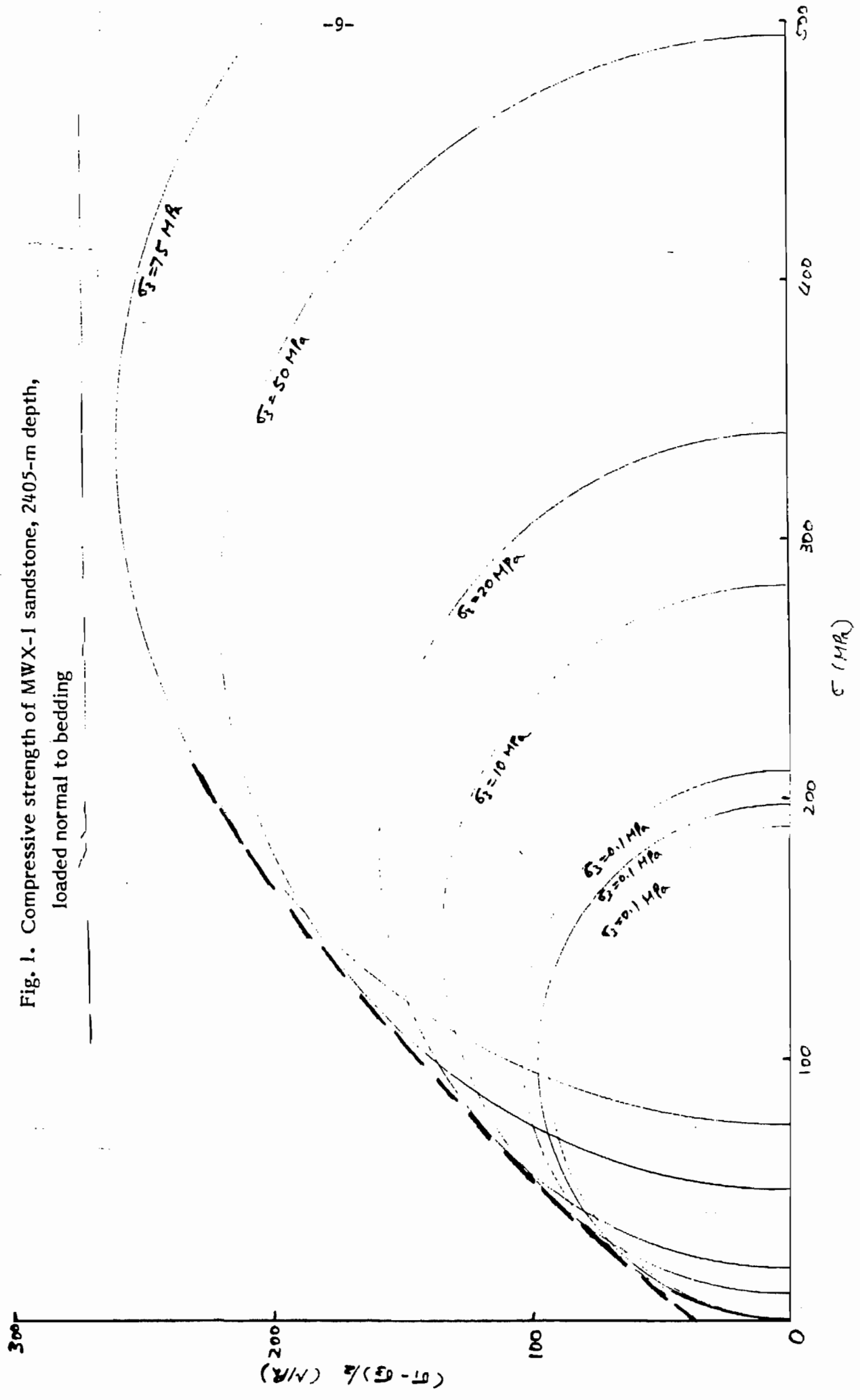
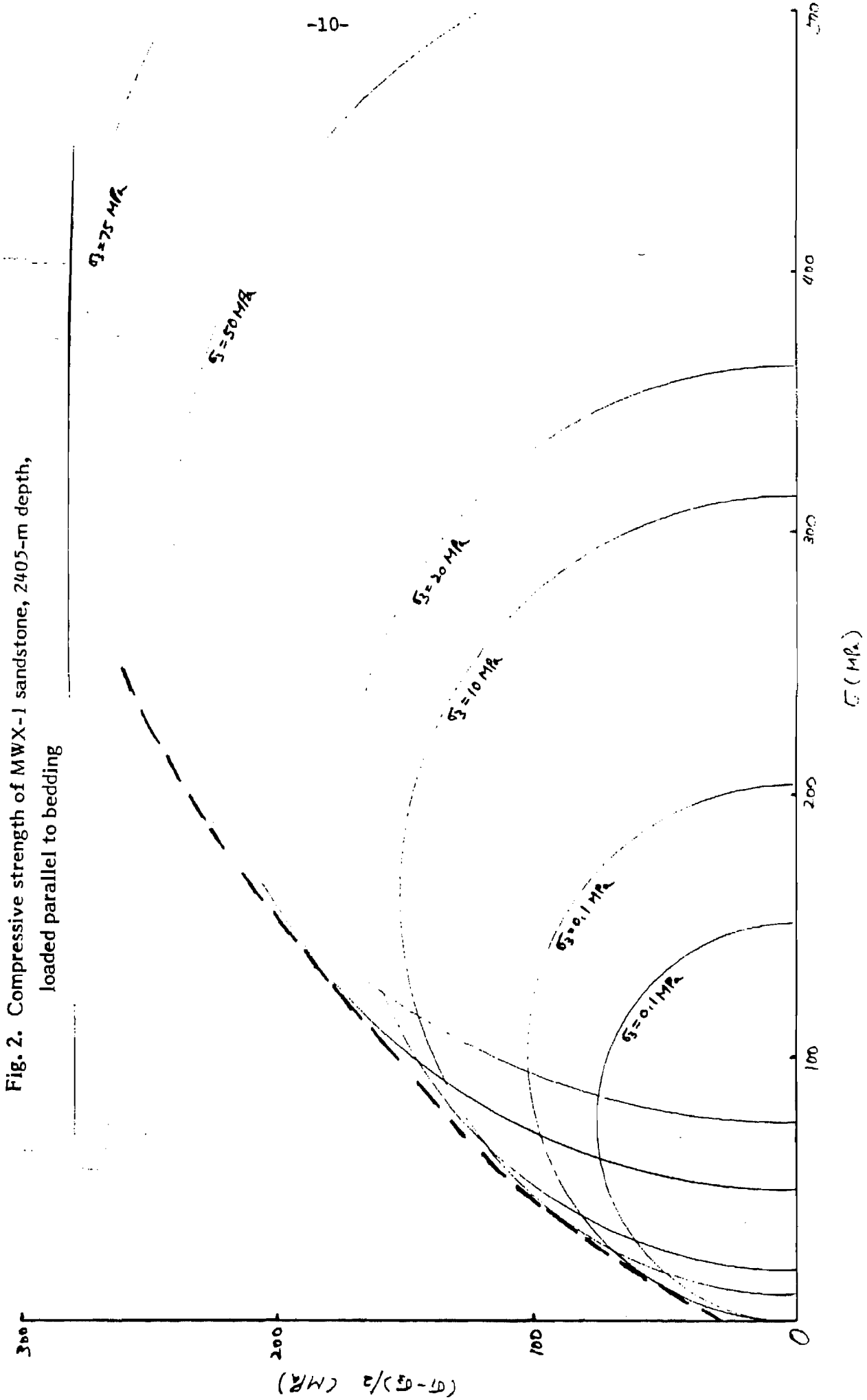


Fig. 2. Compressive strength of MWX-1 sandstone, 2405-m depth, loaded parallel to bedding



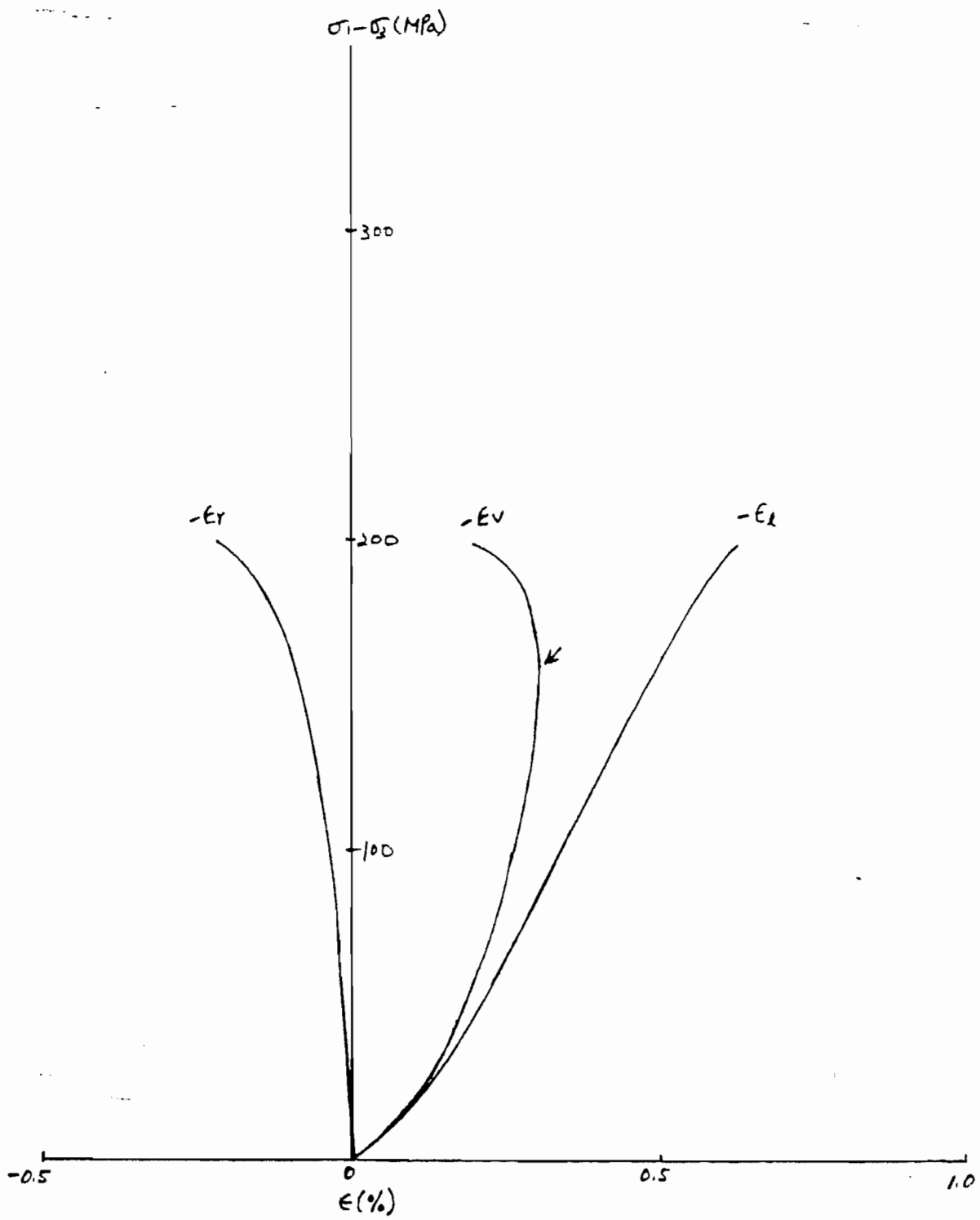


Fig. 3. Stress-strain relation of MWX-1 sandstone, 2405-m depth, loaded normal to bedding at $\sigma_3 = 0.1$ MPa

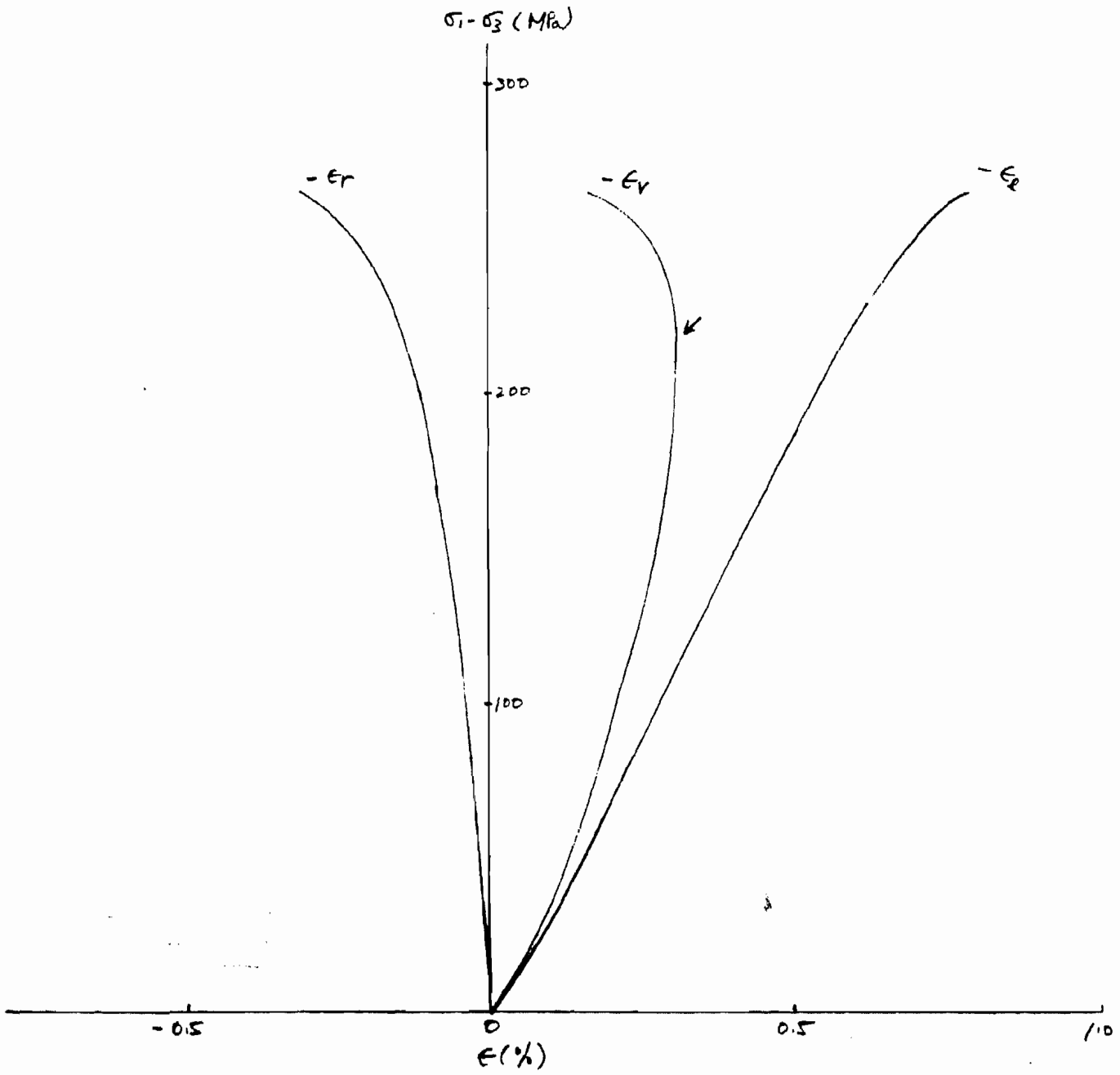


Fig. 4. Stress-strain relation of MWX-1 sandstone, 2405-m depth, loaded normal to bedding at $\sigma_3 = 10$ MPa

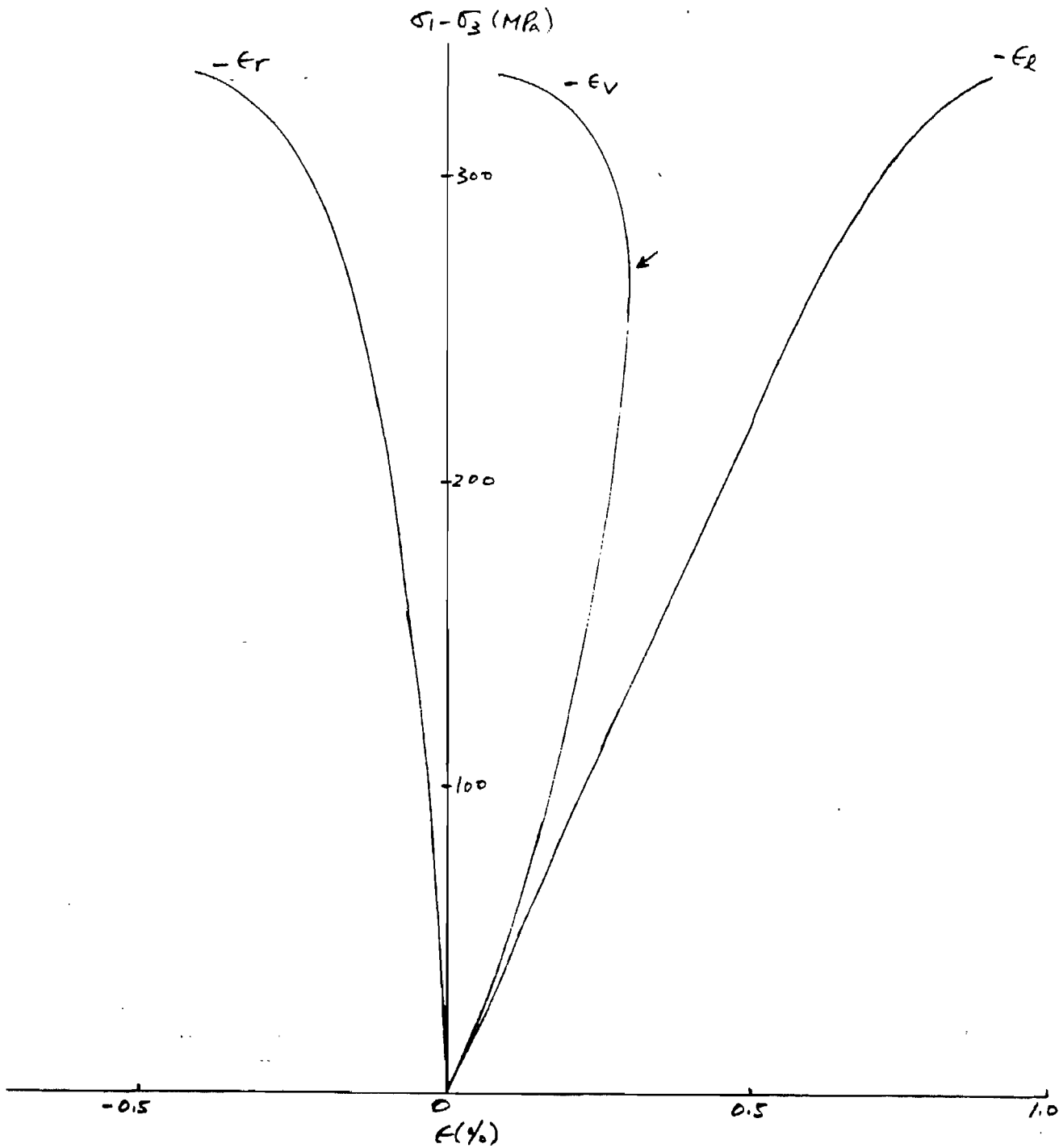


Fig. 5. Stress-strain relation of MWX-1 sandstone, 2405-m depth, loaded normal to bedding at $\sigma_3 = 20$ MPa

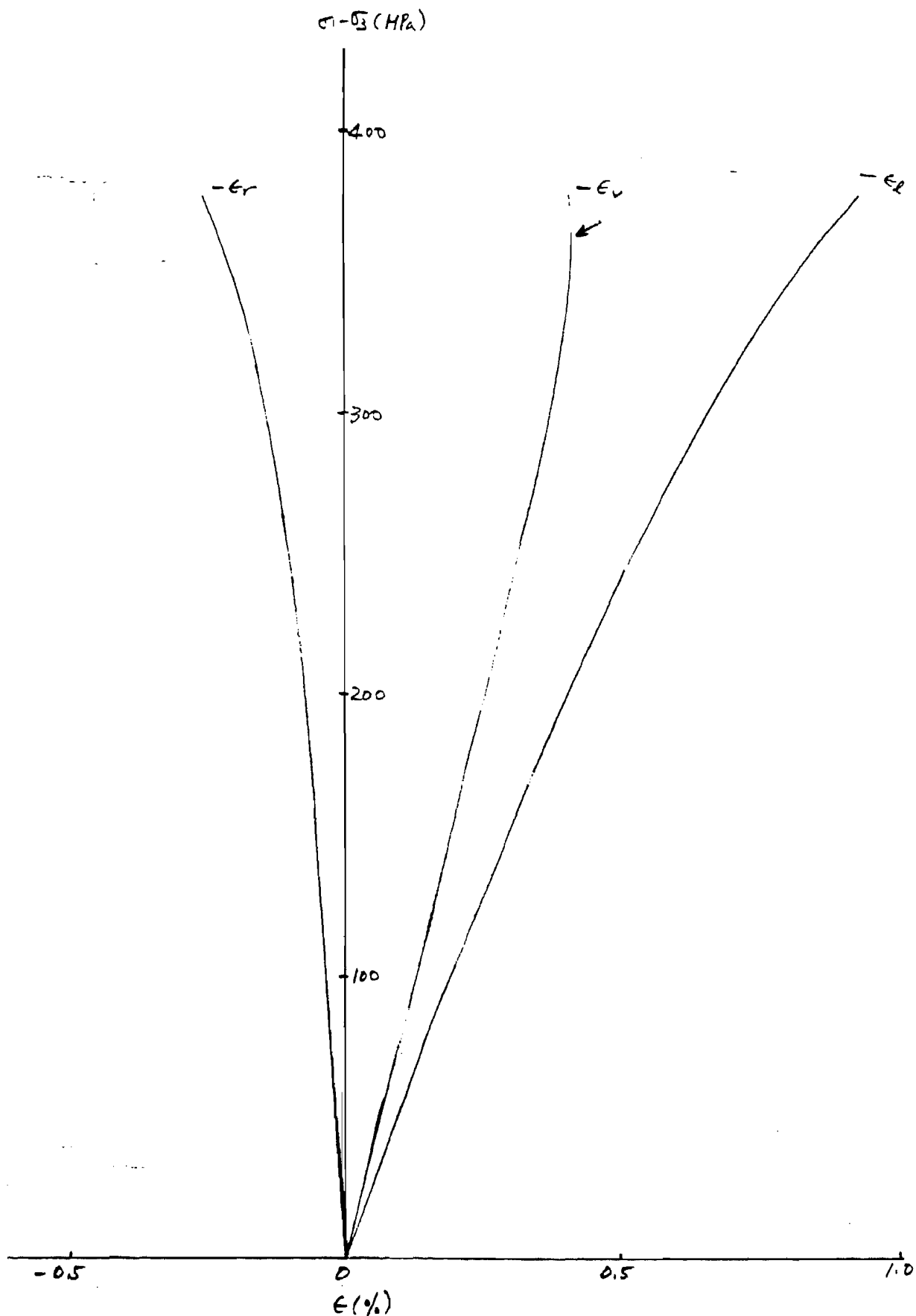


Fig. 6. Stress-strain relation of MWX-1 sandstone, 2405-m depth, loaded normal to bedding at $\sigma_3 = 50$ MPa

Fig. 7. Stress-strain relation of MWX-I sandstone, 2405-m depth,
loaded normal to bedding at $\sigma_3 = 75$ MPa

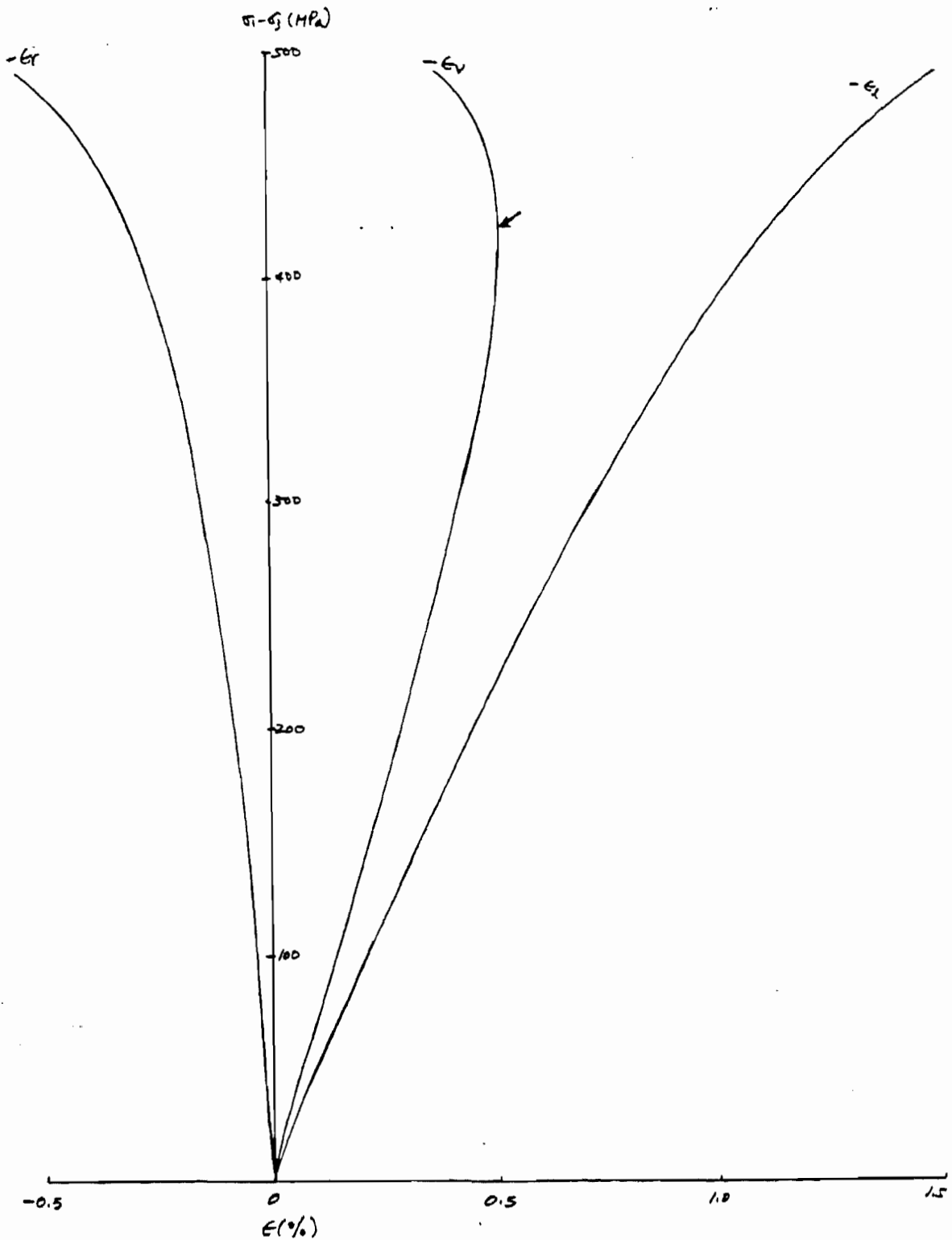


Fig. 8 Stress-strain curve of MWX-1 sandstone, from a depth of 2405 m, loaded parallel to bedding, $\sigma_3 = 0.1$ MPa.

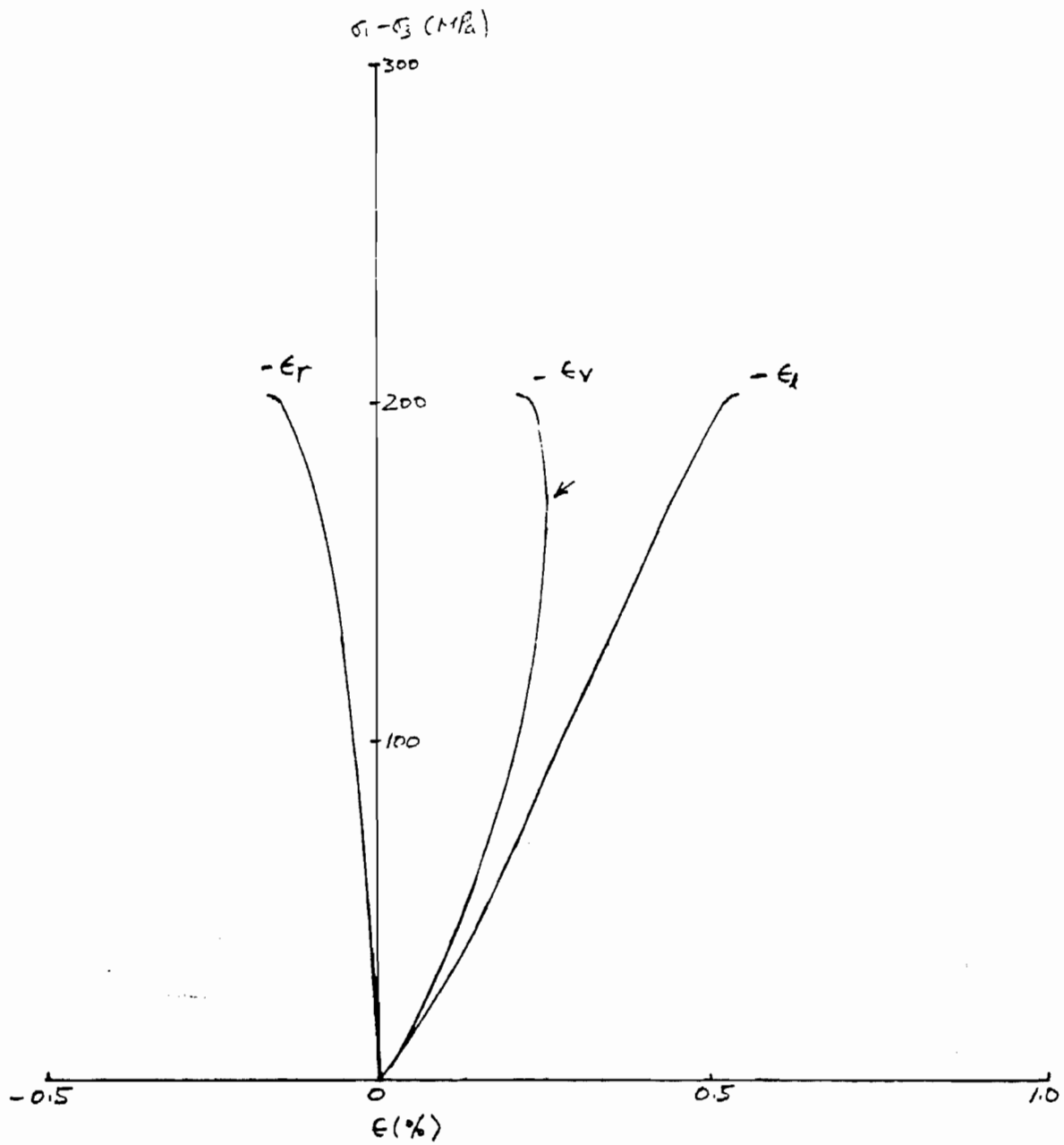


Fig. 9 Stress-strain curves of MWX-1 sandstone, from a depth of 2405 m, loaded parallel to bedding, $\sigma_3 = 10$ MPa.

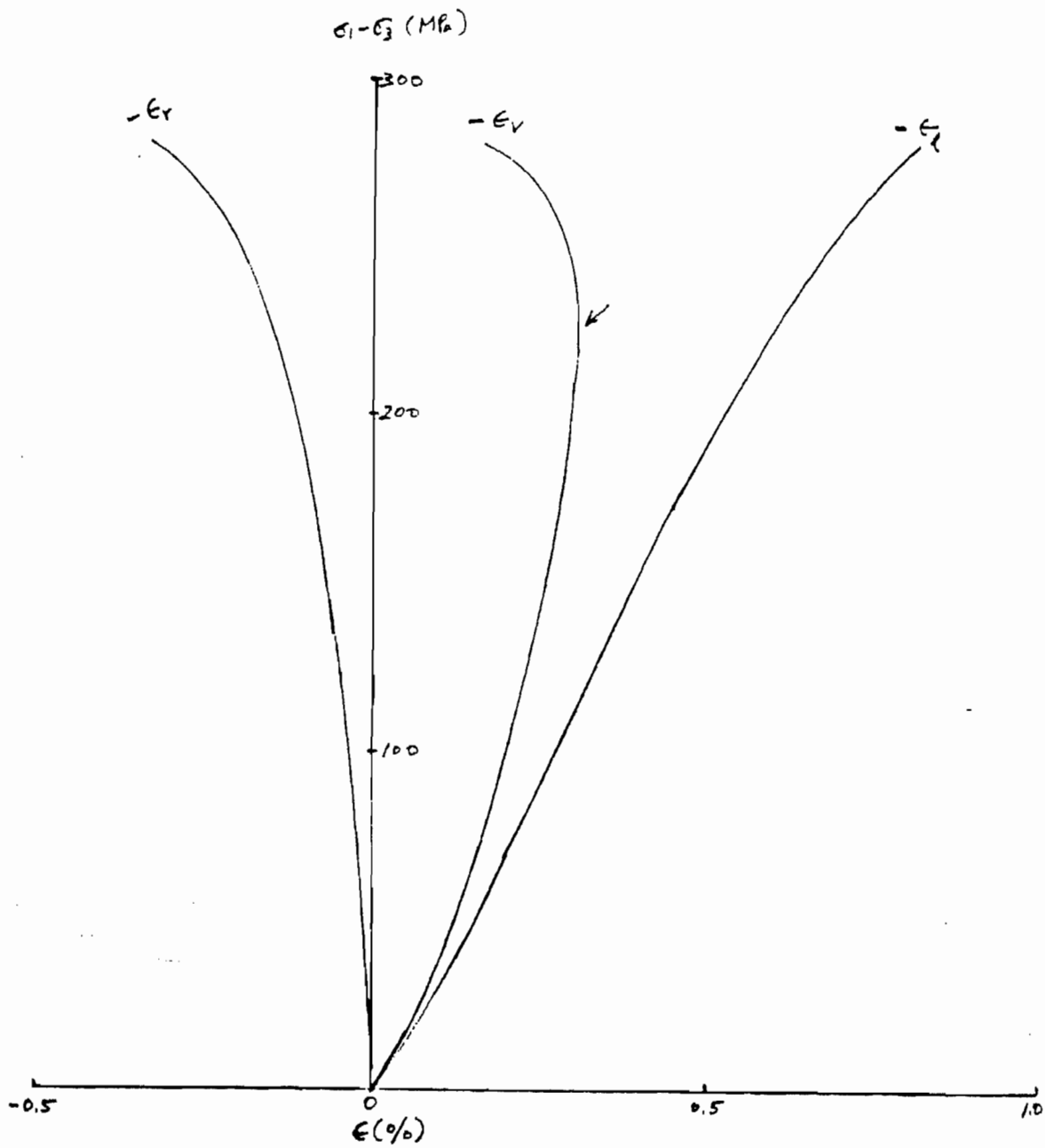
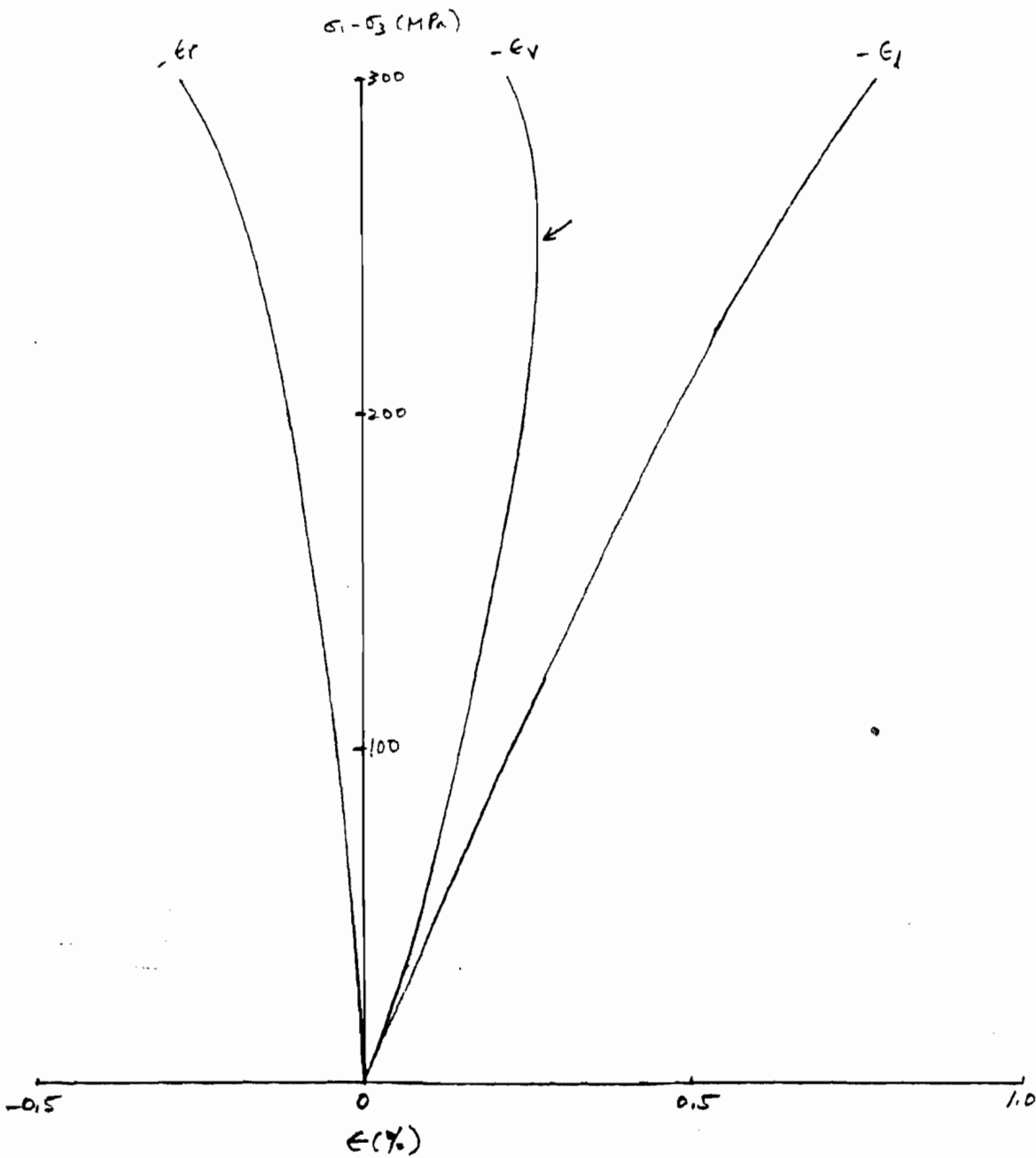


Fig. 10 Stress-strain curves of MWX-1 sandstone, from a depth of 2405 m, loaded parallel to bedding, $\sigma_3 = 20$ MPa



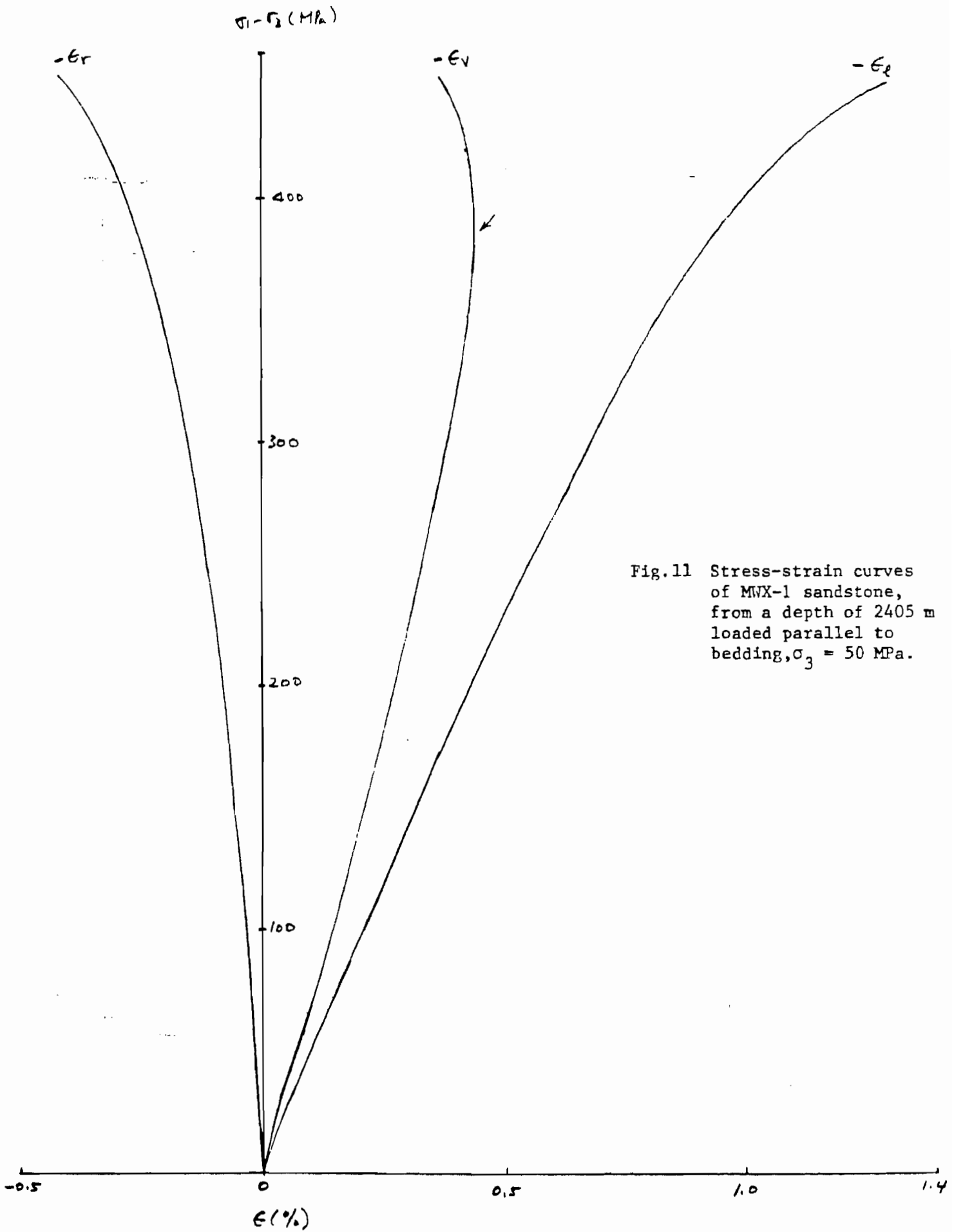


Fig.11 Stress-strain curves of MWX-1 sandstone, from a depth of 2405 m loaded parallel to bedding, $\sigma_3 = 50$ MPa.

Fig. 12. Stress-strain curves of MWX-1 sandstone, from a depth of 2405 m, loaded parallel to bedding, $\sigma_3 = 75$ MPa

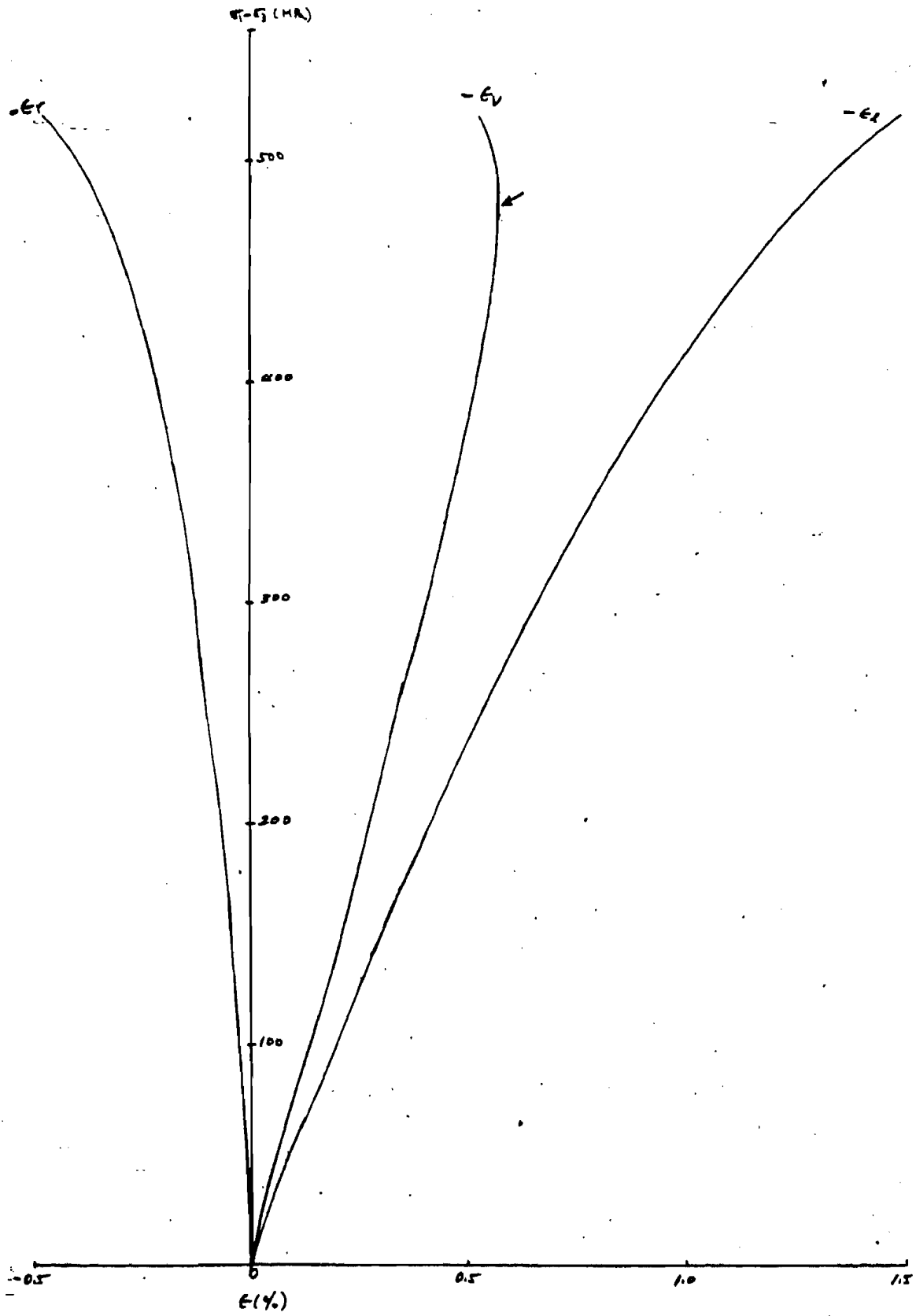


Fig. 13 Hydrostatic compression of MX-1 sandstone, 2405-m depth

